HHS Public Access

Author manuscript

J Immunol. Author manuscript; available in PMC 2016 November 15.

Published in final edited form as:

J Immunol. 2015 November 15; 195(10): 4922–4932. doi:10.4049/jimmunol.1500163.

Novel role of TRPML2 in the regulation of the innate immune response

Lu Sun[1,*], **Yinan Hua**[1,*], **Silvia Vergarajauregui**[1], **Heba I. Diab**[1], and **Rosa Puertollano**[1,#]

[1]Cell Biology and Physiology Center, National Heart, Lung, and Blood Institute, National Institutes of Health, Bethesda, MD, USA

Abstract

TRPMLs (or mucolipins) constitute a family of endosomal cation channels with homology to the transient receptor potential (TRP) superfamily. In mammals, the TRPML family includes three members, TRPML1-3. While TRPML1 and TRPML3 have been well characterized, the cellular function of TRPML2 has remained elusive. To address TRPML2 function in a physiologically relevant cell type, we first analyzed TRPML2 expression in different mouse tissues and organs and found that TRPML2 was predominantly expressed in lymphoid organs and kidney. Quantitative RT-PCR revealed tight regulation of TRPML2 at the transcriptional level. While TRPML2 expression was negligible in resting macrophages, TRPML2 mRNA and protein levels dramatically increased in response to toll-like receptor (TLR) activation both *in vitro* and *in vivo*. Conversely, TRPML1 and TRPML3 levels did not change upon TLR activation. Immunofluorescence analysis demonstrated that endogenous TRPML2 primarily localized to recycling endosomes both in culture and primary cells, in contrast with TRPML1 and TRPML3 that distribute to the late and early endosomal pathway, respectively. To better understand the *in vivo* function of TRPML2 we generated a TRPML2 knockout mouse. We found that the production of several chemokines, in particular CCL2, was severely reduced in TRPML2 knockout mice. Furthermore, TRPML2 knockout mice displayed impaired recruitment of peripheral macrophages in response to intra-peritoneal injections of either LPS or live bacteria, suggesting a potential defect in immune response. Overall, our study reveals interesting differences in the regulation and distribution of the members of the TRPML family and identifies a novel role for TRPML2 in innate immune response.

Introduction

Transient Receptor Potential (TRP) channels constitute a large family of cation channels involved in a variety of physiological functions, particularly in sensory signaling (1, 2). TRPs share a common topology of six-membrane-spanning helices with both the amino- and carboxy-terminal tails oriented toward the cytosol, and the pore located between

[#]Address correspondence to: Rosa Puertollano, Cell Biology and Physiology Center, National Heart, Lung, and Blood Institute, National Institutes of Health, 9000 Rockville Pike, Bldg 50/3537, Bethesda, Maryland 20892, USA. Tel.: +1 (301) 451-2361; FAX: +1 (301) 402-1519; puertolr@mail.nih.gov.

[*]These authors contributed equally to this work

Conflict of interest

The authors declare no competing financial interests.

transmembrane segments 5 and 6. The TRP superfamily is divided into seven subfamilies, one being the mucolipin subfamily (also known as TRPML) (3, 4). In mammals, the TRPML family includes three members, TRPML1, TRPML2, and TRPML3, that share approximately 75% amino acid similarity.

Mutations in TRPML1 cause Mucolipidosis type IV (MLIV) (5–7), an autosomal recessive disease characterized by mental and psychomotor retardation, diminished muscle tone (hypotonia), decreased gastric acid (achlorhydria), and visual problems including corneal clouding, retinal degeneration, sensitivity to light, and strabismus (8–12). Meanwhile, a gain-of-function mutation in TRPML3 results in the murine varitint-waddler (Va) phenotype, which is characterized by hearing loss, vestibular dysfunction (circling behavior, head- bobbing, waddling), and coat color dilution (13). In contrast, no clinically significant mutations in TRPML2 have been reported.

TRPMLs display some unique properties. While most TRPs function at the cell surface responding to changes in the extracellular environment, TRPMLs localize to endo/lysosomal organelles. Specifically, TRPML1 localizes primarily to late endosomes/lysosomes (14–16). Several groups have suggested that TRPML1-mediated release of intra-lysosomal calcium is critical in regulating lysosomal fusion with different intraorganellar compartments, including autophagosomes (17), phagosomes (18) and the plasma membrane (19, 20). TRPML1 has also been implicated in lysosomal acidification (21), lysosomal iron release (22), and zinc homeostasis (23). In contrast to the ubiquitous distribution of TRPML1, high levels of TRPML3 expression appear to be restricted to specific cell types, including melanocytes, hair cells of the inner ear, and neonatal enterocytes (24, 25). TRPML3 distributes at the plasma membrane, as well as the earlier compartments of the endocytic pathway (early and late endosomes) (26, 27). Overexpression of TRPML3 causes severe alterations of the endosomal pathway, including enlargement and clustering of endosomes, delayed Epidermal Growth Factor (EGF) receptor degradation, and impaired autophagosome maturation (26, 27). In addition, inhibition of TRPML3 function results in increased accumulation of endosomal luminal calcium, impaired endosomal acidification, and aberrant endosome fusion (28).

While the channel properties and function of TRPML1 and TRPML3 are well established, those of TRPML2 are far less characterized. Work in *drosophila* S2 cells revealed that the TRPML2 channel displays nonselective cation permeability, which is Ca^{2+}–permeable and is inhibited by low extracytosolic pH (29). Also, quantitative RT-PCR analysis showed that TRPML2 mRNA is expressed at very low level in most organs with the exception of thymus, spleen and, to a lesser degree, kidney (30). The lack of reliable antibodies against endogenous TRPML2 has complicated the study of the intracellular distribution of this protein. Our group has previously reported that heterologously expressed TRPML2 mainly localized to Arf6-regulated recycling endosomes in HeLa cells (31). Moreover, expression of a TRPML2 dominant-negative mutant significantly impaired the recycling of internalized glycosylphosphatidylinositol-anchored proteins back to the plasma membrane (31).

In this study, we sought to better understand the physiological function of TRPML2 *in vivo*. For this we first analyzed the expression of TRPML2 in different tissues and cell types and

found that the levels of TRPML2 are dramatically up-regulated in macrophages upon toll-like receptor activation. Generation of a TRPML2 knockout mouse confirmed a novel role of TRPML2 in the innate immune response.

Materials and Methods

Mice and Tissue Preparation

C57BL/6, C57BL/6-Cre mice were purchased from Jackson Laboratory. To generate TRPML2 knockout mice, we purchased mouse embryonic stem (ES) cells containing the *Trpml2*$^{tm1e(KOMP)Wtsi}$ allele (clone EPD0300_5_B06) from the UC Davis KOMP Repository. This non-conditional potential allele has a trapping cassette "SA-βgeo-pA" (splice acceptor-beta-geo-polyA) flanked by flippase recombinase (Flp) target FRT sites upstream of exon4, resulting in truncation of the endogenous transcript and thus creating a constitutive null mutation. The cassette also tags the gene with a lacZ reporter. The FRT flanked region is followed by a promoter driven neo cassette that is floxed by two loxp sites and can be further removed by the Cre recombinase to achieve a “clean” knockout. The ES cells were injected into C57BL/6 blastocysts. These blastocysts were then implanted into the uterus of swiss-webster strain female mice to complete the pregnancy. Chimeric mice were born and crossed with B6 albino for offspring that are all black. These black mice are heterozygous and inbred to produce TRPML2 KO mice.

Mice were genotyped by long range PCR (LRPCR) following the protocol of the IKMC project 37138 (http://www.mousephenotype.org/martsearch_ikmc_project/martsearch/ikmc_project/37138). The two primer pairs used are LAR3 5’-CAC AAC GGG TTC TTC TGT TAG TCC-3’and GF3 5’-CTC TGA GTT CGT AAG CGA GCG AGC-3’; RAF5 5’-CAC ACC TCC CCC TGA ACC TGA AAC-3’ and GR3 5-GAA GAG AGC ATC AGA ATA CTT GGA CAA CAG-3’. After successful identification of TRPML2 KO mice, the colony was maintained by genotyping using the following primer mix for PCR: FRT-F 5’-GTA TAG GAA CTT CGT CGA GAT AAC-3’, M2–5F 5’-CTC AGT GAA CCA AGG AAG GAG AGG-3’ and M2–3R 5’-CTC ATA TGT GGT CCC TTG GCT CTT-3’.

The *Trpml2* $^{flox\text{-}frt\text{-}neo/flox\text{-}frt\text{-}neo}$ mice were crossed with EIIA-Cre mice (Jackson Laboratory, Bar Harbor, ME) to facilitate an *in vivo* neo deletion which generated final “clean” *Trpml2* KO mice. The neo cassette deleted mice were genotyped by two primer pairs: 5’-CAC TTG CTG ATG CGG TGC TGA TTA C-3’ and 5’-GAC ACC AGA CCA ACT GGT AAT GGT AG-3’; and, M2–5F 5’-CTC AGT GAA CCA AGG AAG GAG AGG-3’ and M2–3R 5’-CTC ATA TGT GGT CCC TTG GCT CTT-3’. TRPML2 knockouts were confirmed by RT-qPCR with mouse TRPML2 probes (QT00133434) (Qiagen, Valencia, CA) to detect TRPML2 mRNA expression.

All of the mice were bred and/or maintained in the NHLBI specific pathogen free animal facility. Experiments were performed when mice were 8 to 14 weeks of age under protocols approved by the NHLBI Animal Care and Use Committee.

Macrophage stimulation *in vivo* and *in vitro*

Lipopolysaccharide (LPS) from *Escherichia coli* 0127:B8 was obtained from Sigma, St. Louise (catalog number L3129) and dissolved in saline solution at 100 ng/μl. The LPS solution was sterilized and intraperitoneally injected at a dose of 0.5 μg per gram of body weight. At indicated times, peritoneal cells were harvested by rinsing the peritoneal cavity with 6 ml of HBSS. After washing, cells were stained for FACS experiments or lysed for mRNA and protein assessments.

For *in vivo* macrophage activation with live bacteria, enterotoxigenic *Escherichia coli* (ETEC) strain H10407 was purchase from ATCC (ATCC-35401), and was grown overnight in Luria-Bertani (LB) broth at 37°C. Bacterial was pelleted, washed twice in sterile PBS (sPBS), diluted to 200 μL sPBS containing 5×10^7 colony forming unite (CFU), and subsequently injected intraperitoneally to wild type and TRPML2 knockout mice. The actual CFU was confirmed by serial dilution test on LB agar plate.

RAW 264.7 were cultured in DMEM plus 10% FBS. MH-S cells were cultured in RPMI 1640 with 10% FBS. At indicated times, cultured cells were stimulated with 1 μg/mL of LPS or 0.2 μg/mL of R848 (Enzo, NY).

Cell culture and *in vitro* differentiation

To obtain bone marrow derived macrophage (BMDM), BM cells were isolated from femurs and tibias of 8-week old female mice. Suspended BM cells were cultured in BM differentiation medium: RPMI-1640 supplemented with 10% fetal bovine serum, 100 U/ml penicillin, 100 μg/ml streptomycin, 2 mM L-glutamine and 40 ng/ml recombinant murine M-CSF (Peprotech, Rocky Hill, NJ). Cells were seeded in non-tissue culture treated Petri dishes (BD351029) and incubated at 37°C in a 5% CO_2 atmosphere. Four days after seeding, fresh BM differentiation medium were added to each plate and cells were incubated for an additional three days. To isolate BMDM, supernatants were discarded and attached cells were washed with sterile HBSS. Macrophages were detached by adding 2 ml of cell stripper (Invitrogen) and incubated at 37°C for 5 min.

Alveolar macrophage were obtained by digesting isolated mouse lung tissue with Liberase (0.14 U/ml)(Roche, Germany) at 37°C for 60 min. After digestion, separated cells were washed with RPMI 1640 with 20% FBS and plated onto 10cm culture dishes (BD350003) with 20 ml of RPMI 1640 containing 20% FBS for seven days. Medium was changed at day two. The alveolar macrophages were loosely attached on fibroblast cells and harvested by pipetting with a 1 ml tip.

Microglia cells were extracted from P1 mouse brains. Every four dissected cortices were placed in 15 ml conical tubes with 10 ml of ice cold HBSS for 30 min. After aspirating HBSS, brains were triturated and digested with 4 ml of trypsin/EDTA at 37°C for 15 min. The enzymatic digestion was stopped by adding 4 ml complete microglial media (DMEM with 10% FBS, 0.08% gentamycin). The cells were centrifuged at 1500 rpm for 5 minutes, resuspended in 10 ml microglial complete media, and plated on a 10cm tissue culture dish coated with Poly-D-Lysine. Media was changed at day three and cells were harvested at day ten.

RAW 264.7 cells (ATCC, Manassas, VA) were maintained in DMEM plus 10% FBS. They were split every three days. MH-S cells (ATCC, Manassas, VA) were cultured in RPMI 1640 with 10% FBS. Passage procedure was identical to that of RAW 264.7 cells. All cell lines were incubated at physiologic levels (37°C, 5% CO_2).

Adenovirus

Adenovirus expressing mouse TRPML2 was prepared, amplified, and purified by Welgen Inc.

Flow cytometry

Cell suspensions were preincubated with an antibody specific for mouse $F_C\gamma$II/III (2.4G2, obtained from Harlan, Netherlands) for 10 min on ice. Cells were then stained on ice for 15 min with a cocktail of fixable viability dye (eBioscience, San Diego, CA) and with fluorochrome-conjugated mAbs against several surface markers, including CD11b (M1/70), F4/80 (BM8), CD80 (16-10A1), MHC-I (AF6–88.5.5.3),), Ly-6G (Gr-1), CD16/CD32 (eBioscience, San Diego, CA). Flow cytometry data were collected with LSR II flow cytometer system (BD Biosciences, San Jose, CA) and the results were analyzed using FlowJo software (Tree Star). Peritoneal macrophages were recognized as double positive for CD11b and F4/80. Based on fluorescence intensity, these macrophages included two populations: the resident macrophages (bright for both CD11b and F4/80) and recruited macrophages (dim for the same markers). Peritoneal neutrophils were recognized as double positive for Ly-6G and CD16.

RNA isolation and quantitative RT-PCR

RNA was isolated from cells by using PureLink Total RNA Purification System (Invitrogen, Carlsbad, CA) and following manufacturer recommendations. RNA yield was quantified by measuring the optical density at 260 and 280 nm using an Eppendorf BioPhotometer. 1 μg RNA was reverse transcribed in a 20 μL reaction using oligo(dT)20 and SuperScript III First-Strand Synthesis System (Invitrogen, Carlsbad, CA) following manufacturer recommendations. PCR was performed using 5 μL SYBR GreenER qPCR SuperMix (Invitrogen, Carlsbad, CA), 2 μL cDNA, 1 μL gene specific primer mix (QuantiTect primer Assays, QIAGEN, Valencia, CA) and 2 μL water for a total reaction volume of 10 μL. Quantification of gene expression was performed using 7900HT Fast Real-Time PCR System (Applied Biosystems, Carlsbad, CA). The thermal profile of the reaction was: 50°C for 2 min, 95°C for 10 min and 40 cycles of 95°C for 15 seconds followed by 60°C for 1 min. All samples were run in triplicates. Amplification of the sequence of interest was compared with a reference probe (mouse β-Actin, QT01136772) and normalized against a standard curve of cell line mRNA. The 7900HT Fast Real-Time PCR System Software was used for data analyses (Applied Biosystems, Carlsbad, CA).

Western blotting

Lysates were collected by resuspending cells in lysis buffer (25 mm Hepes-KOH, pH 7.4, 250 mm NaCl, 1% Triton X-100 (wt/v) supplemented with protease inhibitors cocktail), passing through a 25 gauge needle, and collecting soluble fractions after centrifugation.

Samples were analyzed by SDS-PAGE (4–20% gradient gels) under reducing conditions and transferred to nitrocellulose. Membranes were immunoblotted using the indicated antibodies. Horseradish peroxidase-chemiluminiscence was developed by using Western Lightning Chemiluminescence Reagent Plus (PerkinElmer Life Sciences, Bridgeville, PA).

TRPML2 antibody was generated by injecting GST-N terminal TRPML2 (39 amino acids) fusion protein into rabbits (Pierce, Rockford, IL), and purified from day 72 bleeding serum. The DNA sequence coding mouse TRPML2 N-terminal 39 amino acids was amplified by PCR. The primers used were: 5'-AAT AATGGA TCC TCA TGC CCG GAG ACG AG-3' and 5'-ATT ATG CGG CCG CTC ACT CTT CCC TCA CCT C-3'. The PCR was digested by restriction enzyme and inserted into PGEX-5×1 vector BamHI/NotI site. The plasmid construct was transfected into Rosetta 2 (Millipore, Billerica, MA) competent cells, and GST fusion protein was induced by 100 μM IPTG at 30°C overnight. The GST-N terminal TRPML2 was purified by using Glutathione Sepharose beads (GE Healthcare, Milwaukee, WI) and injected into rabbits. The rabbit serum was sequentially purified by Affi-Gel10 columns pre-conjugated with GST and GST-TRPML2 proteins (BioRad, Hercules,CA). Mouse anti-actin was purchased from BD biosciences.

Confocal microscopy

Macrophages attached to coverslip were fixed in 4% paraformaldehyde (PFA) and permeabilized with 0.2% Triton X-100 at room temperature for 10 min. Coverslips were then incubated with specific first antibodies diluted in immunostaining solution (0.1% Saponin, 1% FBS in PBS) for 1hr at room temperature followed by incubatin with a fluorophore conjugated secondary antibody for 30 min at room temperature. Mouse TRPML2 was stained with rabbit polyclonal anti-TRPML2 first antibody, followed by Alexa488 or Alexa568-labeled Goat anti-Rabbit IgG (Molecular probe, Eugene, OR). Transferrin receptor was recognized by mouse anti-TfR Ab (clone H68.4) (Invitrogen, #13–6800) followed by Alexa488 or Alexa568-labeled goat anti-mouse IgG. LAMP1 was first stained with Rat anti-Mouse LAMP1 (1D4B from DSHB, Iowa city, IA), followed by Alexa488-labeled Donkey anti-Rat IgG. Giantin polyclonal antibody was from Covance (PRB-114C), CCL2 mouse monoclonal antibody (clone 2D8) was from EMDmillipore (MABN712). Images were acquired by confocal microscopy (LSM 510 META; Zeiss) with a 63× Plane Apochromat objective lens (NA 1.4).

Macrophage infection and CFU assay

M. smegmatis (strain ATCC 700084/ mc(2)155) were grown in Middlebrook 7H9 medium enriched with 10% (v/v) albumin/dextrose/catalase (ADC; ATCC) for liquid growth. Equal number of lung macrophages from WT and TRPML2 KO mice were plated in 24-well plates and infected with *M. smegmatis*. After infection for 1 hour, cells were washed with PBS and lysed with sterilized water. 100 μl lysates were growing in LB broth. The broth were performed by 10-fold serial dilutions and inoculated on agar plates incubated at 37°C. The number of colonies was counted at indicated time and referred to as colony forming units (CFU).

Cytokine array panel

Cultured bone marrow derived macrophage (BMDM) from WT and TRPML2 knockout mice were left untreated or incubated with LPS for 24 hours. Cell culture supernatants were collected and centrifuged to remove particulates. 100 μl of supernatant was immediately assayed. To collect cell lysates, BMDM were solubilized in lysis buffer (1% Igepal CA-631, 20 mM Tris-HCl (pH8), 137 mM NaCl, 10% glycerol, 2 mM EDTA, and protease inhibitor) at 4°C for 30 min. 25 μl of cell lysate was used for the assay. Cytokine levels in BMDM supernatants and lysates were assessed using the Proteome Profiler Mouse Cytokine Array kit, Panel A (R&D, Minneapolis, MN).

Measurement of CCL2 content in BMDM culture supernatants by ELISA

Cell culture supernatants from WT or TRPML2$^{-/-}$ BMDM were collected and used for CCL2 measurement by using an ELISA kit from R&D systems (MJE00) per manufacturer's instruction. Cell culture supernatants were diluted by 5 times for the assay. 50 μL diluted supernatants were assessed.

Statistics

Groups were compared with Prism 6 software (GraphPad) using a 2-tailed unpaired Student's t test or two-way ANOVA. Data are presented as mean ± SEM. $P < 0.05$ was considered significant.

Results

TRPML2 mRNA levels are up-regulated in macrophages upon toll-like receptor activation

To better understand TRPML2 function in a physiologically relevant cell type, we analyzed TRPML2 expression in a series of mouse tissues and organs by quantitative RT-qPCR. In agreement with previous studies, we found that TRPML2 mRNA is predominantly expressed in lymphoid and kidney organs (Figure 1A). Notably, TRPML2 expression was tightly regulated at the transcriptional level. While TRPML2 was present at very low levels in resting RAW 264.7 macrophages, its expression increased over 20 fold in response to lipopolysaccharide (LPS), an activator of toll-like receptor 4 (TLR4) (Figure 1B). In contrast, the mRNA levels of TRPML1 and TRPML3 did not change upon LPS stimulation (Figure 1C).

TLRs are a family of membrane-spanning innate immune receptors that recognize ligands derived from bacteria, fungi, viruses, and parasites (32, 33). Activation of TLRs leads to a variety of downstream signals that are critical for proper immune response. To confirm upregulation of TRPML2 in response to TLR activation in primary cells we isolated microglia cells from mice and treated them with a panel of TLR activators, including LPS (TLR4), Loxoribine (TLR7), R848 (TLR7 and TLR8), and ZymosanA (TLR2). In all cases, we observed an increase in the levels of TRPML2 upon TLR activation as assessed by quantitative RT-PCR (Figure 1D).

We then evaluated the differential expression of TRPML2 in response to various incubation times with TLR activators. This detailed kinetic analysis revealed that TRPML2 was

significantly up-regulated within the first six hours of activation (Figure 1E–H). In RAW 264.7 cells, TRPML2 levels reached a maximum expression 24 hours after activation with either LPS or R848, and then progressively decreased back to basal levels approximately 72 hours after activation (Figure 1E). In contrast, maximum levels of TRPML2 mRNA expression were achieved six hours after stimulation in a cell line of alveolar macrophages (MH-S) (Figure 1F), as well as in primary bone marrow derived macrophages (BMDM) (Figure 1G) and primary lung macrophages (Figure 1H). Overall, these results show a very pronounce transcriptional upregulation of TRPML2 upon macrophage activation in both culture and primary cells.

Generation of TRPML2 knockout mice

To characterize the role of TRPML2 *in vivo*, we generated TRPML2 knockout mice. TRPML2 null mice were derived from an embryonic stem cell (ES) clonal cell-line obtained from the Knockout Mouse Project (KOMP) Repository. The ES cell-line contains a gene-trap cassette inserted between exons 3 and 4 of the mouse *MCOLN2* gene that results in an early truncation of the protein (Figure 2A). Targeted disruption of TRPML2 was confirmed by quantitative RT-PCR. As seen in Figure 2B, treatment of BMDM with LPS for six hours considerably induced TRPML2 expression, whereas no TRPML2 mRNA was detected in BMDM derived from TRPML2$^{-/-}$ mice.

To further corroborate absence of the TRPML2 protein in our knockout mice, we generated a new antibody capable of detecting endogenous levels of TRPML2. In agreement with our quantitative RT-PCR analysis, we found that the levels of TRPML2 protein were almost negligible in resting BMDM but were dramatically increased upon BMDM activation with LPS (Figure 2C). The predicted molecular weight of mouse TRPML2 is 65 KDa. However, our antibody detected a much higher molecular weight band in activated macrophages. Several studies have reported that heterologously expressed TRPML2 has the ability to form homomultimers as well as heteromultimers with other members of the TRPML family (34). Our results confirm that endogenous TRPML2 predominantly forms multimers in relevant cell types. As shown in Figure 2C, there was a complete absence of TRPML2 protein in BMDM isolated from knockout mice both in resting and activation conditions.

To further confirm that the specificity of our antibody, we infected ARPE-19 cells with either control adenovirus (Ad-Null) or adenovirus encoding untagged mouse TRPML2 (Ad-TRPML2). As expected, our antibody detected TRPML2 monomers and oligomers in cells expressing Ad-TRPML2 but not in cells infected with Ad-Null (Supplementary Figure 1A).

TRPML2 localizes to recycling endosomes in activated macrophages and microglia

To better characterize TRPML2, we next analyzed the intracellular distribution of TRPML2 in macrophages. Expression of Ad-TRPML2 in resting or LPS-activated RAW 264.7 cells revealed that recombinant TRPML2 localized to vesicular structures dispersed throughout the cytoplasm (Figure 3A and Supplementary Figure 1B). Interestingly, we observed a majority of TRPML2-positive structures co-stained with the transferrin receptor (TfR), a marker of recycling endosomes (Figure 3A and Supplementary Figure 1B). Similar results were observed when RAW cells were activated with R848 (Figure 3B).

To confirm upregulation of endogenous TRPML2 in activated primary macrophages, BMDM were incubated with R848 for 24 hours. Treated cells were clearly stained by our anti-TRPML2 antibody, whereas no labeling was observed in untreated cells. We did not detect any positive staining in BMDM derived from TRPML2$^{-/-}$ mice after treatment with R848, thus validating the specificity of our antibody (Figure 3C).

Next we aimed to corroborate the recycling endosome distribution of endogenous TRPML2 in other primary cell types. As seen in Figure 4A, endogenous TRPML2 was detected in primary microglia when cells were treated with LPS for 24 hours. Similar to RAW cells, TRPML2 localized to TfR-positive organelles. Secondly, we isolated lung tissue from wild type mice. These samples included of a mix of alveolar macrophages and fibroblasts. Treatment with LPS led to TRPML2 upregulation in alveolar macrophages (CD11-positive cells) but not in fibroblasts (CD11-negative cells) as analyzed by immunofluorescence (Figure 4B) and quantitative RT-PCR (Figure 4C). Lastly, upregulation of TRPML2 was also observed in alveolar macrophages in response to R848 (Figure 4C and 4D). The majority of TRPML2 vesicles co-localized with TfR (Figure 4D). However, no co-localization with the lysosomal marker LAMP1 was observed (Figure 4D). It is important to note that TfR cycles between recycling endosomes and the plasma membrane. Therefore, in some cells it is not unusual to find this protein both in recycling endosomes (bigger in size and concentrated in the perinuclear area) and early endosomes (smaller in size and distributed more toward the periphery of the cell). As seen in Figure 4D, TRPML2 co-localizes with TfR almost exclusively in perinuclear endosomes. All together, our data show that TRPML2 co-localizes to recycling endosomes in activated macrophages and microglia.

Characterization of TRPML2 knockout mice

TRPML2 knockout mice were obtained with a Mendelian frequency, were fertile, and had no apparent abnormalities by 20 months of age when compared to their wild type (WT) counterparts. To assess growth, body weights (n=8 for each genotype) were measured at regular intervals in both male and females for a period of 20 weeks and then again at 78 weeks. The body weight of TRPML2$^{-/-}$ mice was not different from the body weight of control mice (Supplementary Figure 2).

At 3 and 18 months of age, control and TRPML2$^{-/-}$ mice were compared according to several tests designed to assess muscle, cerebellar, sensory, and neuropsychiatric function. These included SHIRPA (SmithKline Beecham, Harwell, Imperial College, Royal London Hospital, phenotype assessment), open field test, gait analysis, grip strength and rota rod, and modified morris water test. No significant differences were observed between control and knockout mice (data not shown).

Because of the relatively high levels of expression of TRPML2 in kidney (Figure 1A), control and knockout mice were placed in metabolic cages and renal function was assessed. Table 1 summarizes the metabolic cage data obtained and shows that there were no significant differences in baseline values for the examined parameters between wild type and TRPML2 knockout mice.

Altered chemokine secretion in TRPML2$^{-/-}$ mice

The strong transcriptional upregulation of TRPML2 in activated macrophages suggests that TRPML2 might have an important role in the regulation of macrophage activation or function. To address this possibility BMDM from control and TRPML2$^{-/-}$ mice were treated with LPS for different periods of time. No significant differences in the surface levels of F4/80, CD80, and MHCI were observed between control and TRPML2$^{-/-}$ cells, thus suggesting that TRPML2 is not required for the trafficking of these proteins to the plasma membrane (Supplementary Figure 3).

It was previously reported that CG8743, the homolog of TRPMLs in *Drosophila melanogaster*, plays a role in restricting growth of *Mycobacterium smegmatis* in S2 cells, likely by facilitating delivery of the bacteria to lysosomes and subsequent degradation (35). Therefore, we checked whether TRPML2 might play an analogous role to CG8743 in mouse macrophages. Infection of BMDM isolated from control mice with *Mycobacterium smegmatis* substantially induces TRPML2 expression that was maximal four hours post-infection (Figure 5A). This suggested that TRPML2 upregulation occurs, not only in response to purified TLR ligands, but also to live bacteria. However, when analyzed by CFU (colony forming unit), there was no difference in bacterial uptake or growth between control and TRPML2$^{-/-}$ cells; and, most bacteria were degraded after 24 hours (Figure 5B). Moreover, we observed *Mycobacterium smegmatis* delivery to lysosomes in alveolar macrophages isolated from both control and KO mice (Figure 5C). Therefore, it is possible that another member of the TRPML family, most likely TRPML1, accounts for the degradation defect reported in *drosophila* S2 cells (18).

To better understand the potential role of TRPML2 in the immune response, we measured cytokine and chemokine production by using commercially available antibody arrays. BMDM isolated from either wild type or TRPML2$^{-/-}$ mice were treated with LPS for 24 hours. Cell lysates were then collected and incubated with nitrocellulose membranes in which antibodies for forty different cytokines and chemokines had been spotted (cytokine array panels). Interestingly, we found that the levels of specific chemokines (CCL3, CCL5, and CXCL2), as well as the intracellular adhesion molecule-1 (ICAM1 or CD54), were reduced in samples obtained from TRPML2 knockout animals (Figure 6A). This reduction was very consistent when the experiments were repeated using different pairs of wild type and knockout animals (Figure 6B). In addition, we performed a time-course of LPS activation and found that the amount of secreted CCL2 (measured by ELISA) was significantly decreased in TRPML2$^{-/-}$ cell culture supernatants at all time points (Figure 6C). Similar results were obtained by incubating cell supernantants from LPS-treated wild-type and TRPML2$^{-/-}$ BMDM with cytokine array panels (Figure 6D). The reduction in the levels of specific chemokines was not the result of failed induction, as the transcriptional up-regulation of CCL5, CCL3, and CCL2 was not significantly different between wild type and TRPML2$^{-/-}$ following LPS treatment (Supplementary Figure 4).

These results suggest that TRPML2 might play a role in the regulation of trafficking and/or secretion. In agreement with this idea, we found increased accumulation of CCL2 in the Golgi of LPS-treated TRPML2$^{-/-}$ BMDM when compared to wild-type cells (Figure 6E).

Analysis of over 150 randomly selected cells by Pearson's Coefficient revealed that the increased co-localization of CCL2 with the Golgi marker Giantin observed in TRPML2$^{-/-}$ cells was statistically significant (Figure 6F). All together, our data reveal that trafficking of specific chemokines is significantly altered in TRPML2$^{-/-}$ macrophages.

In vivo migration of macrophages is impaired in the absence of TRPML2

Chemokines, in particular CCL2, play a critical role in promoting infiltration and migration of monocytes and macrophages to the sites of inflammation (36). To determine whether the migration of macrophages was altered in TRPML2 knockout mice, we evaluated *in vivo* recruitment of peripheral macrophages in response to intra-peritoneal injections of LPS. Eight hours after LPS injection, cells were collected from the peritoneum and labeled for the macrophage marker F4/80. F4/80-positive cells were then separated into two populations, dim and bright, which have been shown to be indicative of recruited and resident macrophages, respectively (Figure 7A) (37). Notably, macrophage recruitment in response to LPS was markedly reduced in TRPML2 knockout mice (Figure 7B). In contrast, the number of resident macrophages was comparable between control and knockout mice (data not shown). Migration of neutrophils to the intraperitoneal space was also significantly decreased in TRPML2$^{-/-}$ animals (Figure 7C). Measurement of TRPML2 mRNA and protein levels in peritoneal macrophages confirmed upregulation of TRPML2 in response to LPS *in vivo* (Figure 7D and 7E).

To further confirm the physiological relevance of our observations, we injected mice intraperitoneally with live enterotoxigenic *Escherichia coli* (ETEC) strain H10407, and measured migration of macrophages and neutrophils into the intraperitoneal space at 8h after the administration of the live bacteria. As expected, we found a very significant delay in both, macrophage and neutrophil migration in TRPML2$^{-/-}$ animals (Figure 7F and 7G). All together, out data reveal a novel role of TRPML2 in the regulation of the innate immune response.

Discussion

In this study we describe, for the first time, a role for TRPML2 in immune response. TRPML2 mRNA and protein levels were dramatically upregulated in culture and primary macrophages upon TLR activation. The increased expression of TRPML2 upon activation of different TLRs indicates that TRPML2 might participate in the host defense against different types of microbial pathogens, including bacteria (recognized by TLR4) and viruses (recognized by TLR7, and TLR8). Recent evidence suggests that the expression of other TRPMLs may also be regulated at the transcriptional level. TRPML1 is upregulated following activation of the transcription factors EB (TFEB) and E3 (TFE3) (38, 39). TFEB and TFE3 translocate to the nucleus upon nutrient deprivation and induce expression of a complex gene network, thus leading to autophagy activation and lysosomal biogenesis (40). It has been proposed that the increased levels of TRPML1 in response to TFEB/TFE3 activation are critical in facilitating fusion of autophagosomes with lysosomes and, in some cases, may also mediate fusion of lysosomes with the plasma membrane (20). Likewise, TRPML3 is highly expressed in neonatal enterocytes, where it plays an important role in the

digestion of maternal-provided nutrients by regulating fusion/fission events between late endosomes/lysosomes, while it is absent in mature intestinal enterocytes (25).

Most studies addressing the intracellular distribution of TRPMLs have relied upon over-expression of recombinant proteins. The low TRPML expression in basal conditions may explain the difficulty of generating antibodies capable of detecting endogenous protein levels. Our results suggest that visualization of endogenous TRPMLs may require analyzing specific cell types or activation conditions. For example, we previously described that heterologously expressed TRPML2 localized primarily to recycling endosomes in HeLa cells. However, under these conditions, some TRPML2-positive staining was also observed at plasma membrane and lysosomes. The extensive co-localization with transferrin receptor, reveals that, al least in activated macrophages and microglia, endogenous TRPML2 distributes almost exclusively to recycling endosomes. In addition, it has been suggested that TRPML1 and TRPML3, both of which localize to early/late endosomal compartments, might be redundant in some cell types (25). The distinct distribution of TRPML2 in recycling endosomes argues against a possible redundancy between TRPML2 and the other members of the TRPML family.

Work from several laboratories supports the concept that TRPMLs function as calcium release channels that regulates fusion of endosomal organelles with different cellular compartments. In agreement with this idea, we have previously described that in HeLa cells, TRPML2 facilitates trafficking of certain proteins along the recycling pathway (31). Therefore, we propose that increased expression of TRPML2 in activated macrophages might lead to more dynamic vesicular carriers, thus increasing membrane fusion and enhancing protein recycling and/or secretion. Accordingly, we found increased intracellular accumulation and reduced secretion of CCL2 in BMDM isolated from TRPML2 knockout mice. Chemokine/cytokine secretion does not follow a unique trafficking pathway, but rather could involve multiple pathways and organelles depending on whether they get delivered locally or whether the release is more multidirectional on the cell surface. For example, in macrophages, IL-6 and TNF reside in distinct non-overlapping areas of recycling endosomes, suggesting that this compartment may function as a sorting hub for local secretion of cytokines (41). Moreover, in mast cells, CCL2 secretion is inhibited by inactivation of syntaxin 6, a t-SNARE required for fusion of vesicular carriers arriving from the trans-Golgi network (TGN) to recycling endosomes (42). Therefore, TRPML2 could facilitate fusion of recycling endosomes with either TGN-derived carriers or plasma membrane, thus promoting secretion of specific chemokines/cytokines.

It is well established that CCL2 promotes attraction of immune cells to the sites of inflammation. Although we cannot rule out additional defects in TRPML2$^{-/-}$ macrophages, the reduced levels of CCL2 and other migratory chemokines is consistent with the decreased numbers of recruited macrophages observed *in vivo*. In fact, mice deficient in CCL2 receptor show delayed recruitment of F4/80^{dim} macrophages to the lungs upon *Mycobacterium tuberculosis* infection (37). Future studies should address the susceptibility of TRPML2 knockout mice to *Mycobacterium tuberculosis* and other pathogens.

In summary, our work reveals a novel and exciting role for TRPML2 in the regulation of the innate immune response. It also suggests that cells may regulate expression of TRPMLs in response to specific stimuli as a way to enhance specific trafficking pathways.

Supplementary Material

Refer to Web version on PubMed Central for supplementary material.

Acknowledgements

We thank Dr. Chengyu Liu and Dr. Danielle Springer, from the NHLBI Transgenic and Murine Phenotyping Cores, respectively, for assistance.

This project was supported by the Intramural Research Program of the NIH, National Heart, Lung, and Blood Institute (NHLBI).

References

1. Abe K, Puertollano R. Role of TRP channels in the regulation of the endosomal pathway. Physiology. 2011; 26:14–22. [PubMed: 21357899]
2. Venkatachalam K, Montell C. TRP channels. Annual review of biochemistry. 2007; 76:387–417.
3. Puertollano R, Kiselyov K. TRPMLs: in sickness and in health. American journal of physiology. Renal physiology. 2009; 296:F1245–1254. [PubMed: 19158345]
4. Venkatachalam K, Wong CO, Zhu MX. The role of TRPMLs in endolysosomal trafficking and function. Cell calcium. 2014
5. Bargal R, Avidan N, Ben-Asher E, Olender Z, Zeigler M, Frumkin A, Raas-Rothschild A, Glusman G, Lancet D, Bach G. Identification of the gene causing mucolipidosis type IV. Nature genetics. 2000; 26:118–123. [PubMed: 10973263]
6. Bassi MT, Manzoni M, Monti E, Pizzo MT, Ballabio A, Borsani G. Cloning of the gene encoding a novel integral membrane protein, mucolipidin-and identification of the two major founder mutations causing mucolipidosis type IV. American journal of human genetics. 2000; 67:1110–1120. [PubMed: 11013137]
7. Slaugenhaupt SA, Acierno JS Jr, Helbling LA, Bove C, Goldin E, Bach G, Schiffmann R, Gusella JF. Mapping of the mucolipidosis type IV gene to chromosome 19p and definition of founder haplotypes. American journal of human genetics. 1999; 65:773–778. [PubMed: 10441585]
8. Altarescu G, Sun M, Moore DF, Smith JA, Wiggs EA, Solomon BI, Patronas NJ, Frei KP, Gupta S, Kaneski CR, Quarrell OW, Slaugenhaupt SA, Goldin E, Schiffmann R. The neurogenetics of mucolipidosis type IV. Neurology. 2002; 59:306–313. [PubMed: 12182165]
9. Amir N, Zlotogora J, Bach G. Mucolipidosis type IV: clinical spectrum and natural history. Pediatrics. 1987; 79:953–959. [PubMed: 2438637]
10. Berman ER, Livni N, Shapira E, Merin S, Levij IS. Congenital corneal clouding with abnormal systemic storage bodies: a new variant of mucolipidosis. The Journal of pediatrics. 1974; 84:519–526. [PubMed: 4365943]
11. Livni N, Legum C. Ultrastructure of cultured fibroblasts in mucolipidosis type IV. Experimental cell biology. 1976; 44:1–11. [PubMed: 187459]
12. Tellez-Nagel I, Rapin I, Iwamoto T, Johnson AB, Norton WT, Nitowsky H. Mucolipidosis IV. Clinical, ultrastructural, histochemical, and chemical studies of a case, including a brain biopsy. Archives of neurology. 1976; 33:828–835. [PubMed: 187156]
13. Di Palma F, Belyantseva IA, Kim HJ, Vogt TF, Kachar B, Noben-Trauth K. Mutations in Mcoln3 associated with deafness and pigmentation defects in varitint-waddler (Va) mice. Proceedings of the National Academy of Sciences of the United States of America. 2002; 99:14994–14999. [PubMed: 12403827]

14. Pryor PR, Reimann F, Gribble FM, Luzio JP. Mucolipin-1 is a lysosomal membrane protein required for intracellular lactosylceramide traffic. Traffic. 2006; 7:1388–1398. [PubMed: 16978393]
15. Thompson EG, Schaheen L, Dang H, Fares H. Lysosomal trafficking functions of mucolipin-1 in murine macrophages. BMC cell biology. 2007; 8:54. [PubMed: 18154673]
16. Vergarajauregui S, Puertollano R. Two di-leucine motifs regulate trafficking of mucolipin-1 to lysosomes. Traffic. 2006; 7:337–353. [PubMed: 16497227]
17. Vergarajauregui S, Connelly PS, Daniels MP, Puertollano R. Autophagic dysfunction in mucolipidosis type IV patients. Human molecular genetics. 2008; 17:2723–2737. [PubMed: 18550655]
18. Samie M, Wang X, Zhang X, Goschka A, Li X, Cheng X, Gregg E, Azar M, Zhuo Y, Garrity AG, Gao Q, Slaugenhaupt S, Pickel J, Zolov SN, Weisman LS, Lenk GM, Titus S, Bryant-Genevier M, Southall N, Juan M, Ferrer M, Xu H. A TRP channel in the lysosome regulates large particle phagocytosis via focal exocytosis. Developmental cell. 2013; 26:511–524. [PubMed: 23993788]
19. LaPlante JM, Sun M, Falardeau J, Dai D, Brown EM, Slaugenhaupt SA, Vassilev PM. Lysosomal exocytosis is impaired in mucolipidosis type IV. Molecular genetics and metabolism. 2006; 89:339–348. [PubMed: 16914343]
20. Medina DL, Fraldi A, Bouche V, Annunziata F, Mansueto G, Spampanato C, Puri C, Pignata A, Martina JA, Sardiello M, Palmieri M, Polishchuk R, Puertollano R, Ballabio A. Transcriptional activation of lysosomal exocytosis promotes cellular clearance. Developmental cell. 2011; 21:421–430. [PubMed: 21889421]
21. Soyombo AA, Tjon-Kon-Sang S, Rbaibi Y, Bashllari E, Bisceglia J, Muallem S, Kiselyov K. TRP-ML1 regulates lysosomal pH and acidic lysosomal lipid hydrolytic activity. The Journal of biological chemistry. 2006; 281:7294–7301. [PubMed: 16361256]
22. Dong XP, Cheng X, Mills E, Delling M, Wang F, Kurz T, Xu H. The type IV mucolipidosis-associated protein TRPML1 is an endolysosomal iron release channel. Nature. 2008; 455:992–996. [PubMed: 18794901]
23. Kukic I, Lee JK, Coblentz J, Kelleher SL, Kiselyov K. Zinc-dependent lysosomal enlargement in TRPML1-deficient cells involves MTF-1 transcription factor and ZnT4 (Slc30a4) transporter. The Biochemical journal. 2013; 451:155–163. [PubMed: 23368743]
24. Castiglioni AJ, Remis NN, Flores EN, Garcia-Anoveros J. Expression and vesicular localization of mouse Trpml3 in stria vascularis, hair cells, and vomeronasal and olfactory receptor neurons. The Journal of comparative neurology. 2011; 519:1095–1114. [PubMed: 21344404]
25. Remis NN, Wiwatpanit T, Castiglioni AJ, Flores EN, Cantu JA, Garcia-Anoveros J. Mucolipin Co-deficiency Causes Accelerated Endolysosomal Vacuolation of Enterocytes and Failure-to-Thrive from Birth to Weaning. PLoS genetics. 2014; 10:1004833.
26. Kim HJ, Soyombo AA, Tjon-Kon-Sang S, So I, Muallem S. The Ca(2+) channel TRPML3 regulates membrane trafficking and autophagy. Traffic. 2009; 10:1157–1167. [PubMed: 19522758]
27. Martina JA, Lelouvier B, Puertollano R. The calcium channel mucolipin-3 is a novel regulator of trafficking along the endosomal pathway. Traffic. 2009; 10:1143–1156. [PubMed: 19497048]
28. Lelouvier B, Puertollano R. Mucolipin-3 regulates luminal calcium, acidification, and membrane fusion in the endosomal pathway. The Journal of biological chemistry. 2011; 286:9826–9832. [PubMed: 21245134]
29. Lev S, Zeevi DA, Frumkin A, Offen-Glasner V, Bach G, Minke B. Constitutive activity of the human TRPML2 channel induces cell degeneration. The Journal of biological chemistry. 2010; 285:2771–2782. [PubMed: 19940139]
30. Samie MA, Grimm C, Evans JA, Curcio-Morelli C, Heller S, Slaugenhaupt SA, Cuajungco MP. The tissue-specific expression of TRPML2 (MCOLN-2) gene is influenced by the presence of TRPML1. Pflugers Archiv : European journal of physiology. 2009; 459:79–91. [PubMed: 19763610]
31. Karacsonyi C, Miguel AS, Puertollano R. Mucolipin-2 localizes to the Arf6-associated pathway and regulates recycling of GPI-APs. Traffic. 2007; 8:1404–1414. [PubMed: 17662026]

32. Beutler B. Inferences, questions and possibilities in Toll-like receptor signalling. Nature. 2004; 430:257–263. [PubMed: 15241424]

33. Janssens S, Beyaert R. Role of Toll-like receptors in pathogen recognition. Clinical microbiology reviews. 2003; 16:637–646. [PubMed: 14557290]

34. Venkatachalam K, Hofmann T, Montell C. Lysosomal localization of TRPML3 depends on TRPML2 and the mucolipidosis-associated protein TRPML1. The Journal of biological chemistry. 2006; 281:17517–17527. [PubMed: 16606612]

35. Philips JA, Porto MC, Wang H, Rubin EJ, Perrimon N. ESCRT factors restrict mycobacterial growth. Proceedings of the National Academy of Sciences of the United States of America. 2008; 105:3070–3075. [PubMed: 18287038]

36. Bose S, Cho J. Role of chemokine CCL2 and its receptor CCR2 in neurodegenerative diseases. Archives of pharmacal research. 2013; 36:1039–1050. [PubMed: 23771498]

37. Peters W, Cyster JG, Mack M, Schlondorff D, Wolf AJ, Ernst JD, Charo IF. CCR2-dependent trafficking of F4/80dim macrophages and CD11cdim/intermediate dendritic cells is crucial for T cell recruitment to lungs infected with Mycobacterium tuberculosis. Journal of immunology. 2004; 172:7647–7653.

38. Martina JA, Diab HI, Lishu L, Jeong AL, Patange S, Raben N, Puertollano R. The nutrient-responsive transcription factor TFE3 promotes autophagy, lysosomal biogenesis, and clearance of cellular debris. Science signaling. 2014; 7:9.

39. Sardiello M, Palmieri M, di Ronza A, Medina DL, Valenza M, Gennarino VA, Di Malta C, Donaudy F, Embrione V, Polishchuk RS, Banfi S, Parenti G, Cattaneo E, Ballabio A. A gene network regulating lysosomal biogenesis and function. Science. 2009; 325:473–477. [PubMed: 19556463]

40. Settembre C, Di Malta C, Polito VA, Garcia Arencibia M, Vetrini F, Erdin S, Erdin SU, Huynh T, Medina D, Colella P, Sardiello M, Rubinsztein DC, Ballabio A. TFEB links autophagy to lysosomal biogenesis. Science. 2011; 332:1429–1433. [PubMed: 21617040]

41. Manderson AP, Kay JG, Hammond LA, Brown DL, Stow JL. Subcompartments of the macrophage recycling endosome direct the differential secretion of IL-6 and TNFalpha. The Journal of cell biology. 2007; 178:57–69. [PubMed: 17606866]

42. Frank SP, Thon KP, Bischoff SC, Lorentz A. SNAP-23 and syntaxin-3 are required for chemokine release by mature human mast cells. Molecular immunology. 2011; 49:353–358. [PubMed: 21981832]

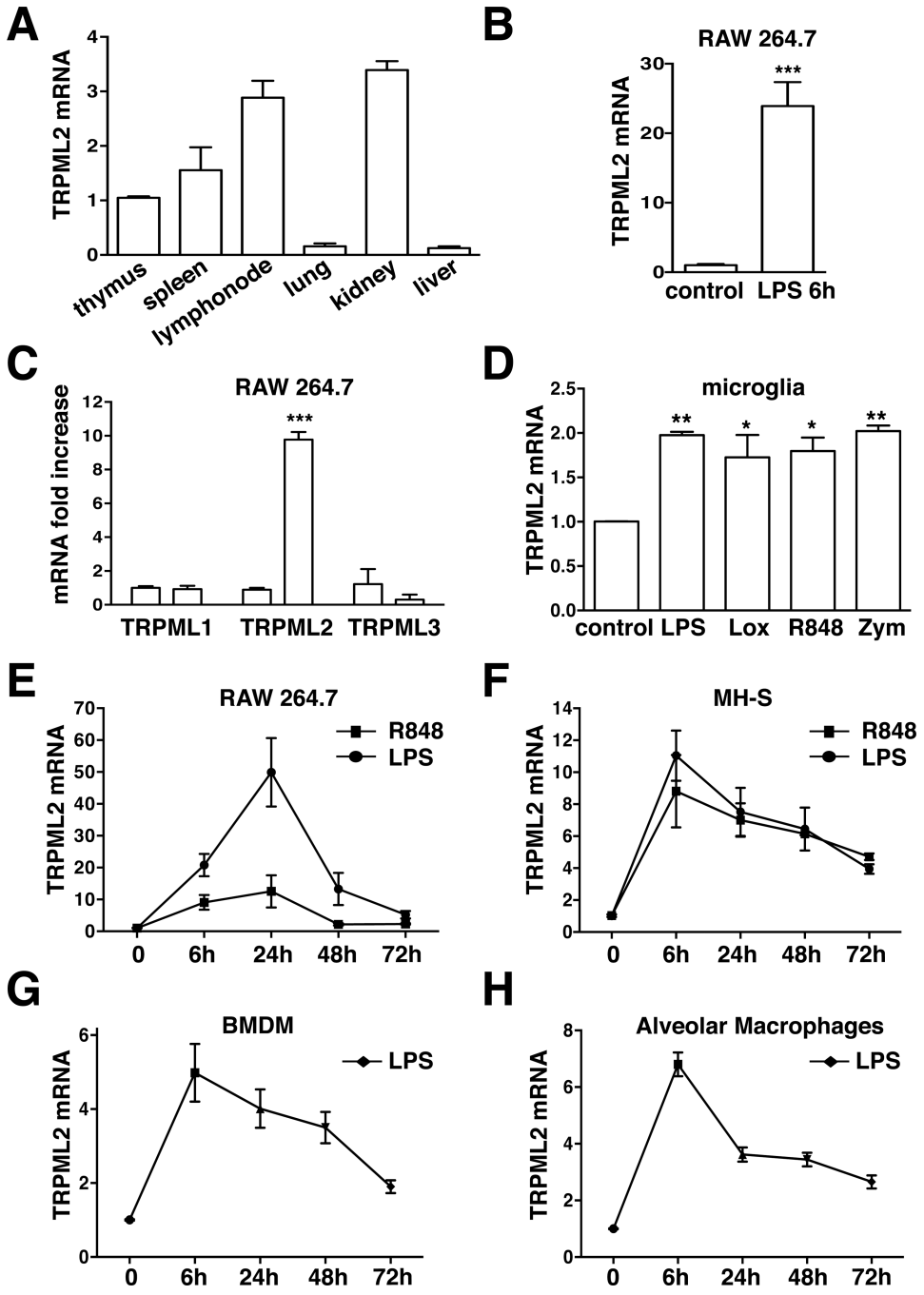

Figure 1. TRPML2 is transcriptionally up-regulated in activated macrophages

A. Measurement of TRPML2 mRNA levels from different C57BL/6N mice organs by quantitative RT-qPCR. TRPML2 mRNA levels were normalized to TRPML2 levels in thymus and represent fold change. Data are presented as means ± SD of four (thymus, liver) or three (spleen, lymphonode, lung, kidney) independent experiments. **B and C.** RAW 264.7 cells were left untreated or incubated with 1μg/ml LPS for 6 hours. Cells were then collected and TRPML2 (B) or TRPML1-3 (C) mRNA levels were measured by RT-qPCR (n=20, ***P< 0.0001). **D.** Transcriptional up-regulation of TRPML2 in microglia in response to

various TLR activators. Cultured microglia cells were treated with the following reagents for 6 hours: LPS (1 μg/ml, TLR4 ligand), Loxoribine (100 nM, TLR7 ligand), R848 (200 ng/ml, TLR7 and TLR8 ligand), and ZymosanA (50 μg/ml, TLR2 ligand). Data are presented as means ± SD of three independent experiments (*$P \leq 0.05$, **$P \leq 0.01$). **E, F.** TRPML2 mRNA levels time course upon LPS and R848 stimulation for 6 hours in RAW 264.7 (n=14) and MH-S (n=9) cells. **G, H.** TRPML2 mRNA levels time course in cultured primary macrophages. Data is presented as mRNA fold change for in bone marrow derived macrophages (n=6) and alveolar macrophages (n=5) 6 hours after LPS treatment.

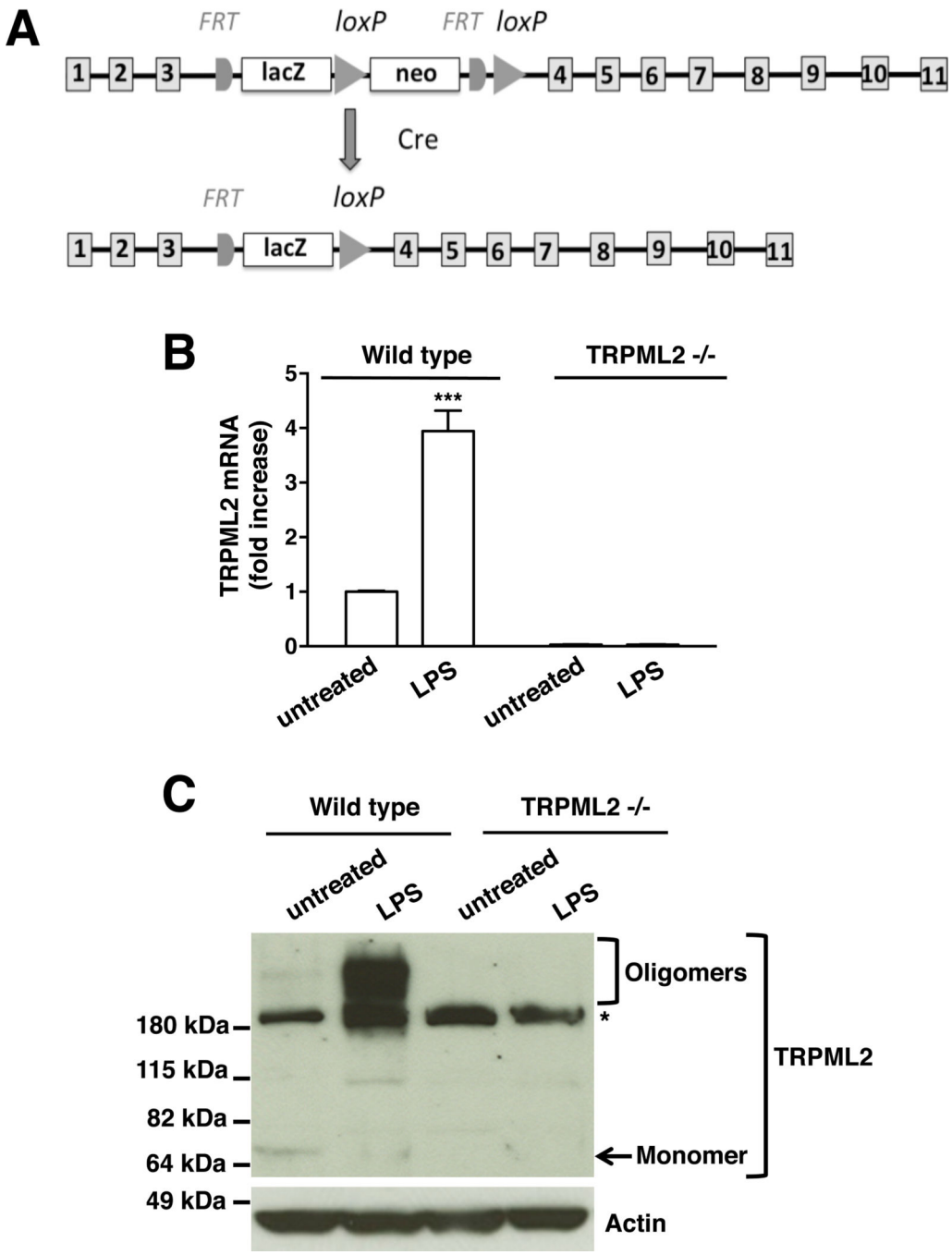

Figure 2. Generation of TRPML2$^{-/-}$ knockout mice

A. Schematic representation of Cre-loxP mediated deletion of TRPML2. The 'knockout-first' allele contains a trapping cassette with a lacZ reporter and a floxed promoter-driven neo cassette inserted into the intron of the *MCOLN2* gene thereby disrupting gene function. By crossing with the EIIA-Cre mouse, the neo cassette between two LoxP sites was deleted. **B.** BMDM extracted from wild type and TRPML2 knockout (KO) mice (n=9) were left untreated or incubated with LPS (1 μg/ml) for 6 hours. TRPML2 mRNA levels from all groups were normalized to the WT untreated samples. Data is presented as mRNA fold

change for four independent experiments (***$P < 0.0001$). **C.** Primary bone marrow macrophages from WT and KO mice were left untreated or treated with LPS (1 μg/ml) for 24 hours. TRPML2 protein levels were assessed by western blotting using rabbit anti-TRPML2 antibody. The results shown are representative of three independent experiments. The predicted molecular weight for TRPML2 is approximately 65 kDa (arrow). TRPML2 oligomers run above the 180 kDA marker. The asterisk indicates an unspecific band recognized by our antibody. Actin (42 kDa) was used as a loading control.

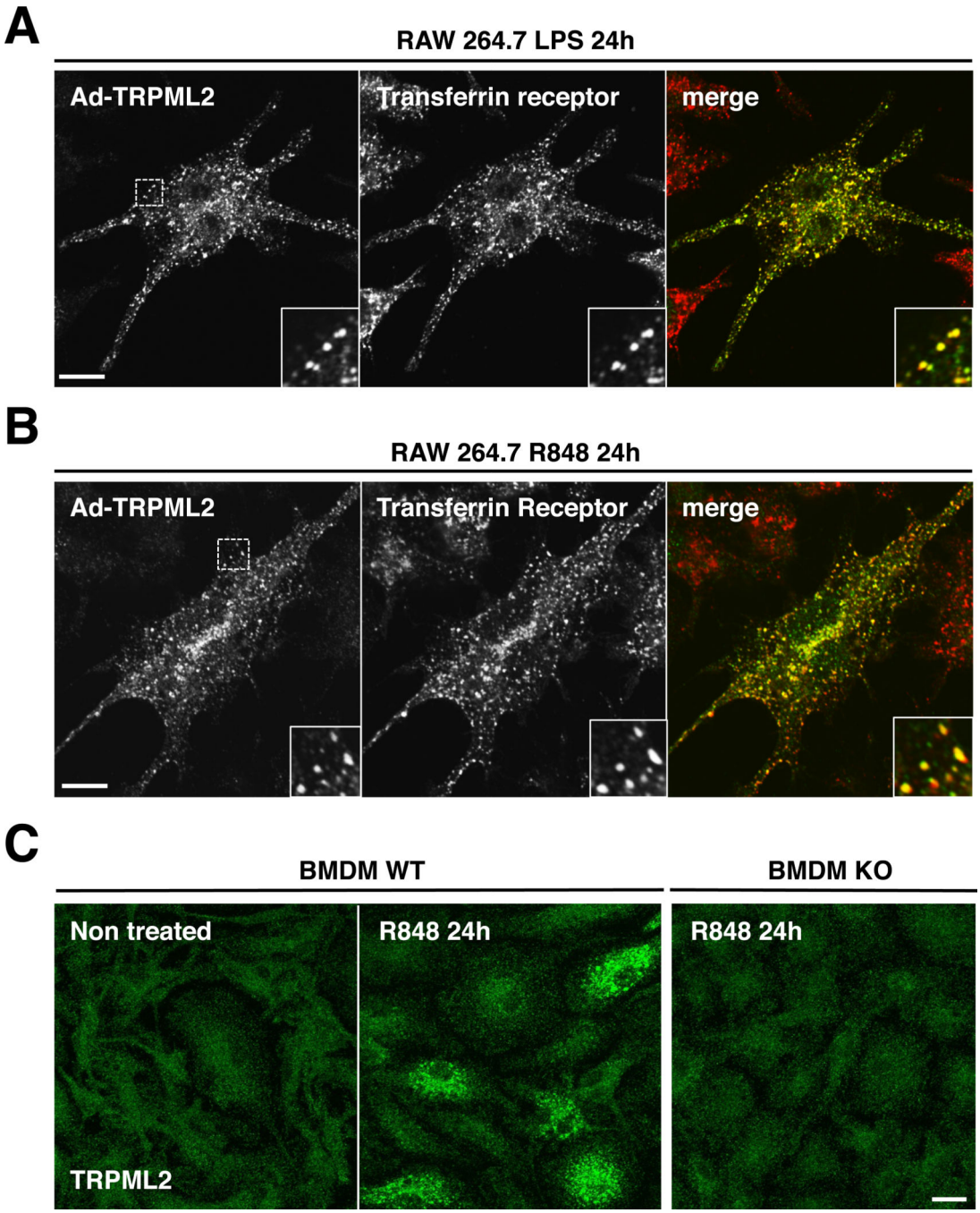

Figure 3. Intracellular distribution of TRPML2 in RAW 264.7 and BMDM

A, B. RAW 264.7 cells were infected with Ad-TRPML2 and stimulated with LPS (1 μg/ml) or R848 (200 ng/ml) for 24 hours. Cells were permeabilized and immunostained with TRPML2 and transferrin receptor (TfR) antibodies and analyzed by confocal fluorescence microscopy. Yellow indicates colocalization between TRPML2 (green) and TfR (red). Insets show a 4-fold magnification of the indicated region. Scale bars, 10 μm. Images are representative of three independent experiments. **C.** WT and TRPML2 KO BMDM were treated with R848 for 24 hours. Endogenous TRPML2 expression was assessed using our

TRPML2 antibody. Scale bars, 10 μm. Images are representative of three independent experiments.

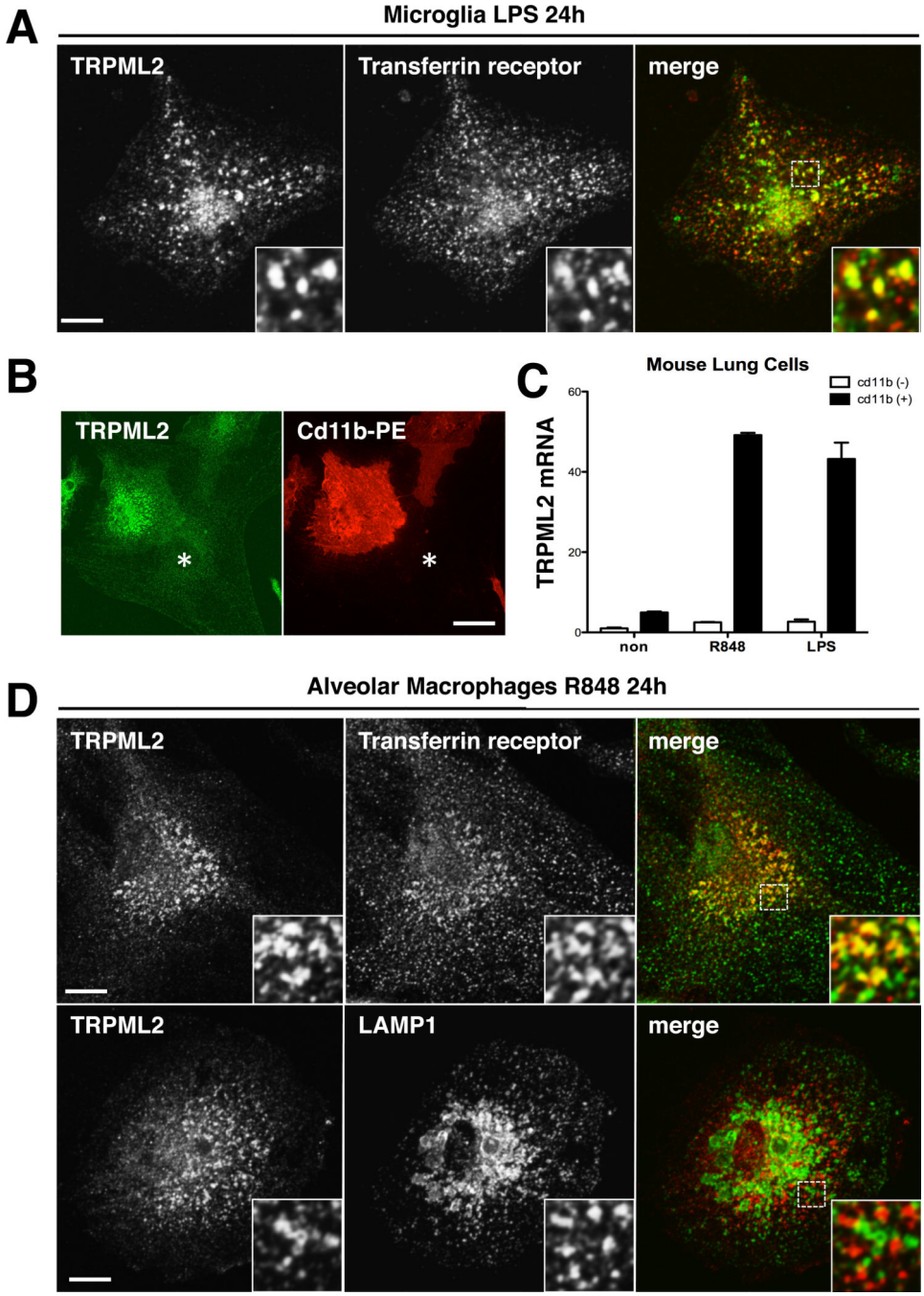

Figure 4. Endogenous TRPML2 localizes to recycling endosomes in activated microglia and alveolar macrophages

A. LPS increases TRPML2 protein levels in primary mouse microglia. Primary microglia cells isolated from wild type mice were treated with LPS (1 μg/ml) for 24 hours. Cells were permeabilized and immunostained with TRPML2 (green) and TfR (red) antibodies. Insets show a 4-fold magnification of the indicated region. Scale bars, 10 μm. Images are representative of three independent experiments **B.** Cultured primary lung cells were stimulated with R848 (200 ng/ml) for 24 hours. TRPML2 expression was detected in

alveolar macrophages ($CD11b^+$) but not in fibroblasts (*). **C.** Cultured lung cells were treated with R848 (200 ng/ml) or LPS (1 μg/ml) for 10 hours and sorted based on CD11b level. **D.** Alveolar macrophages were treated with R848 (200 ng/ml) for 24 hours and immunostained with TRPML2 (red) and TfR or LAMP1 (green) antibodies. Yellow indicates colocalization between TRPML2 and TfR (top) or TRPML2 and LAMP1 (bottom). Insets show a 4-fold magnification of the indicated region. Scale bars, 10 μm. Images are representative of three independent experiments.

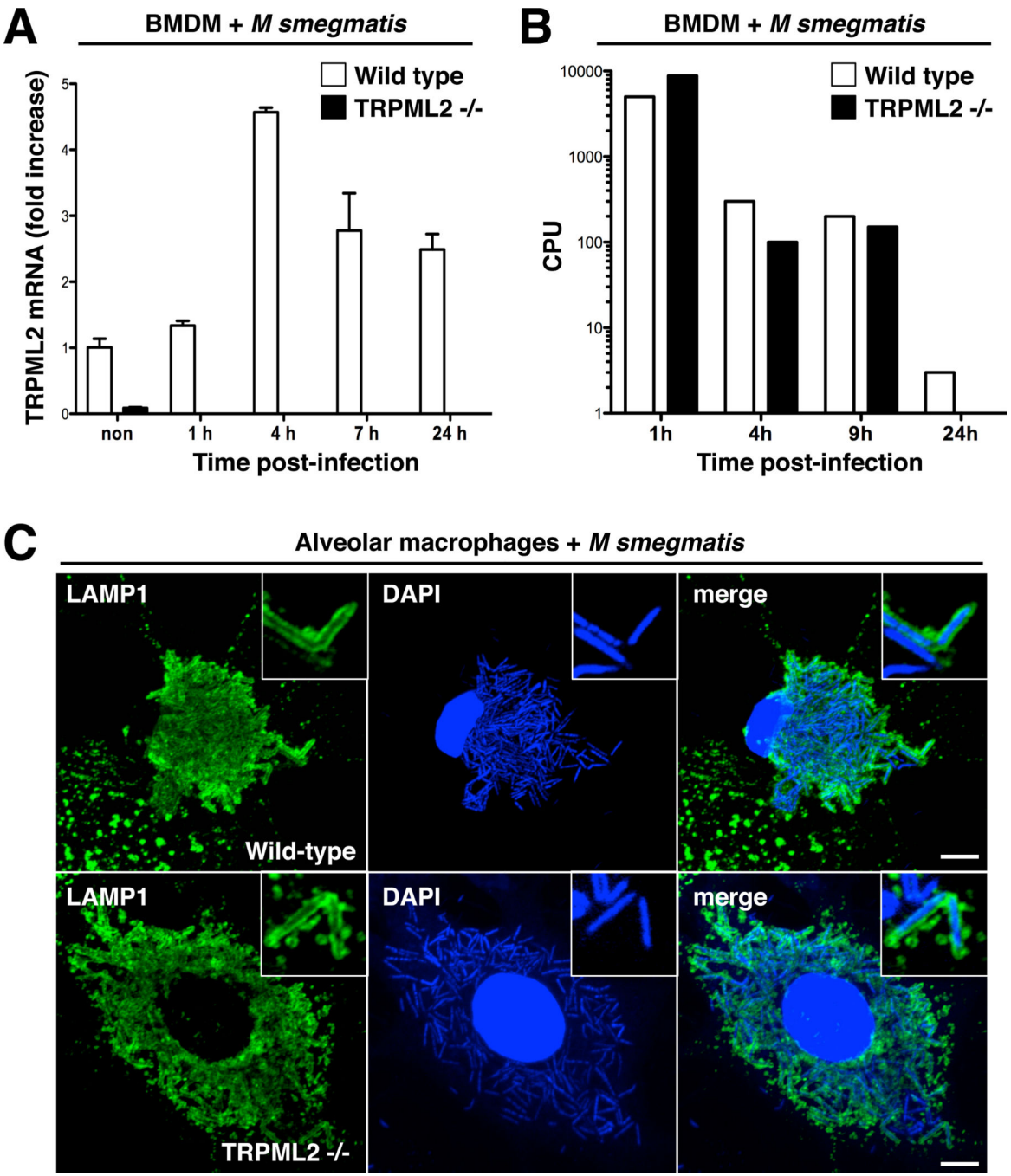

Figure 5. *M. Smegmatis* degradation in alveolar macrophages does not require TRPML2

A. *M. Smegmatis* infection induced TRPML2 mRNA levels in BMDM derived from wild type mice. Equal number of macrophages from WT and TRPML2 KO mice were plated and infected with same amount of *M. smegmatis*. Cells were collected at indicated time points and TRPML2 mRNA was measured by RT-PCR. **B.** The efficiency of WT and TRPML2 KO BMDM to eliminate engulfed *M. smegmatis* was measured as Colony Forming Unit (CFU). Cultured BMDM were infected with *M. smegmatis* at a 1 to 100 ratio (MOI 100). Infected macrophages were lysed at indicated time points. Cell lysates were resuspended in

800ul of LB broth and subjected to serial dilution. Ten microliters of each dilution were plated on LB agar plates. After overnight incubation, the numbers of bacterial colonies were counted. **C.** Infected alveolar macrophages were fixed and stained with LAMP1 antibody (green) and DAPI (blue). The inset shows tubular lysosome surrounding *M. smegmatis* in both WT and KO macrophages. Insets show a 4-fold magnification of the indicated region. Scale bars, 5 μm. Images are representative of three independent experiments.

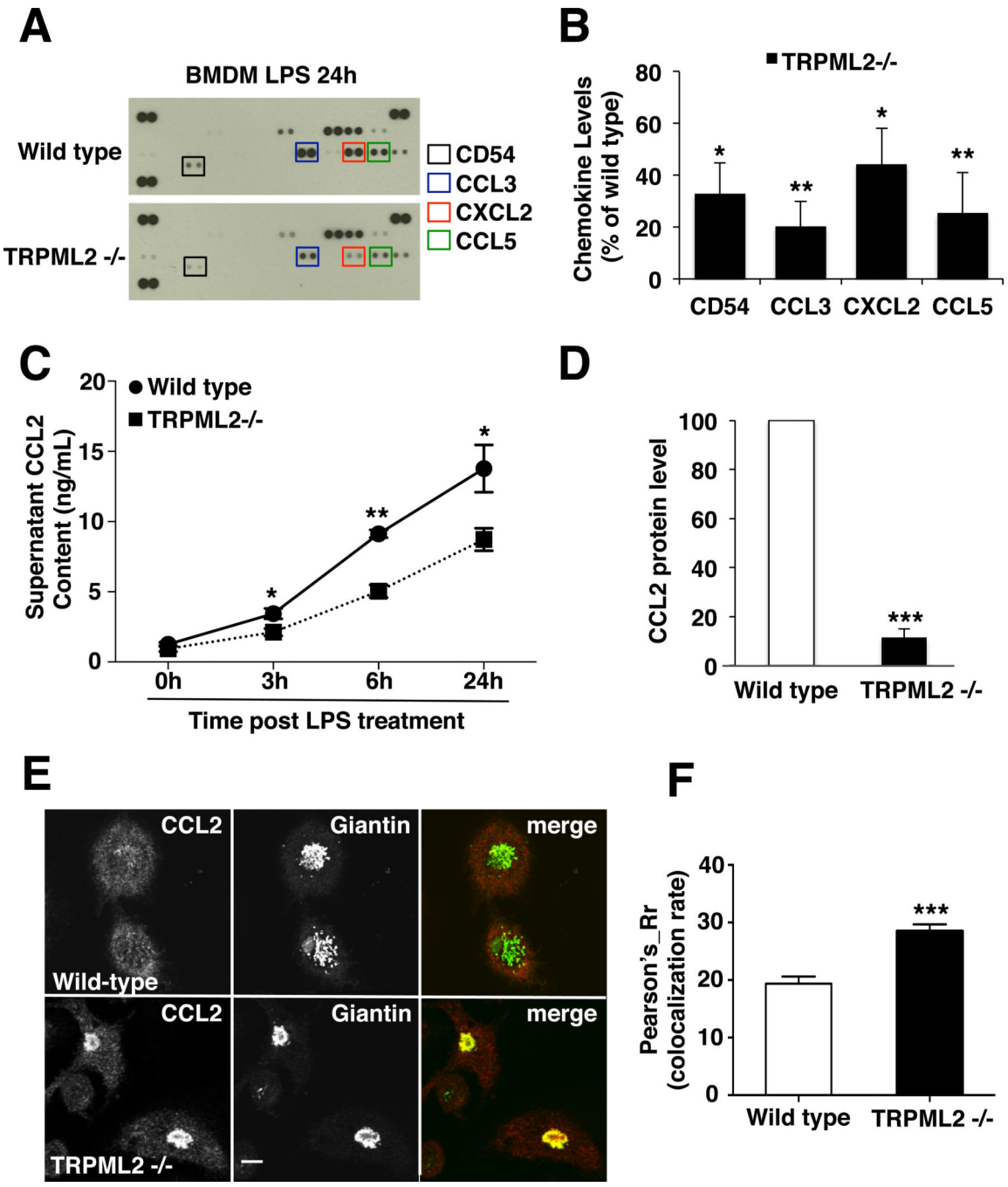

Figure 6. Chemokine secretion is reduced in TRPML2 knockout mice

A. BMDM from WT and TRPML2 KO mice were treated with LPS for 24 hours. Cell lysates were extracted and analyzed using the Proteome Profiler Mouse Cytokine Array from R&D Systems. Blots are representative of three independent experiments. **B.** Spot intensities from the blots in *A* were quantified using ImageJ. Data are presented as the mean percent change of lysate cytokine levels in TRPML2 KO compared to WT ± SEM of three independent experiments. The data were analyzed using Student's t-test (*$P \leq 0.01$, **$P \leq 0.001$). **C.** BMDM from WT and TRPML2 KO mice were treated with LPS for the indicated

times. The CCL2 content in cell supernatants was analyzed by ELISA. Data is presented as mean ± SEM of five independent experiments. The data were analyzed using Student's t-test (*$P \leq 0.05$, **$P \leq 0.005$). **D.** BMDM from WT and TRPML2 KO mice were treated with LPS for 24 hours. The cytokine content in culture supernatants was analyzed as in *A*. Data is presented as the mean percent change of serum cytokine levels in TRPML2 KO compared to WT ± SEM of three independent experiments. The data were analyzed using Student's t-test (***$P \leq 0.0005$). **E.** BMDM cells isolated from wild type and TRPML2 KO mice were treated with LPS (1 μg/ml) for 24 hours. Cells were permeabilized and immunostained with CCL2 (red) and Giantin (green) antibodies. Scale bars, 10 μm. Images are representative of three independent experiments. **F.** Co-localization between CCL2 and Giantin in LPS-treated wild-type (n=154) and TRPML2$^{-/-}$ (n=169) BMDM was quantified by Pearson's coefficient (***$P \leq 0.005$).

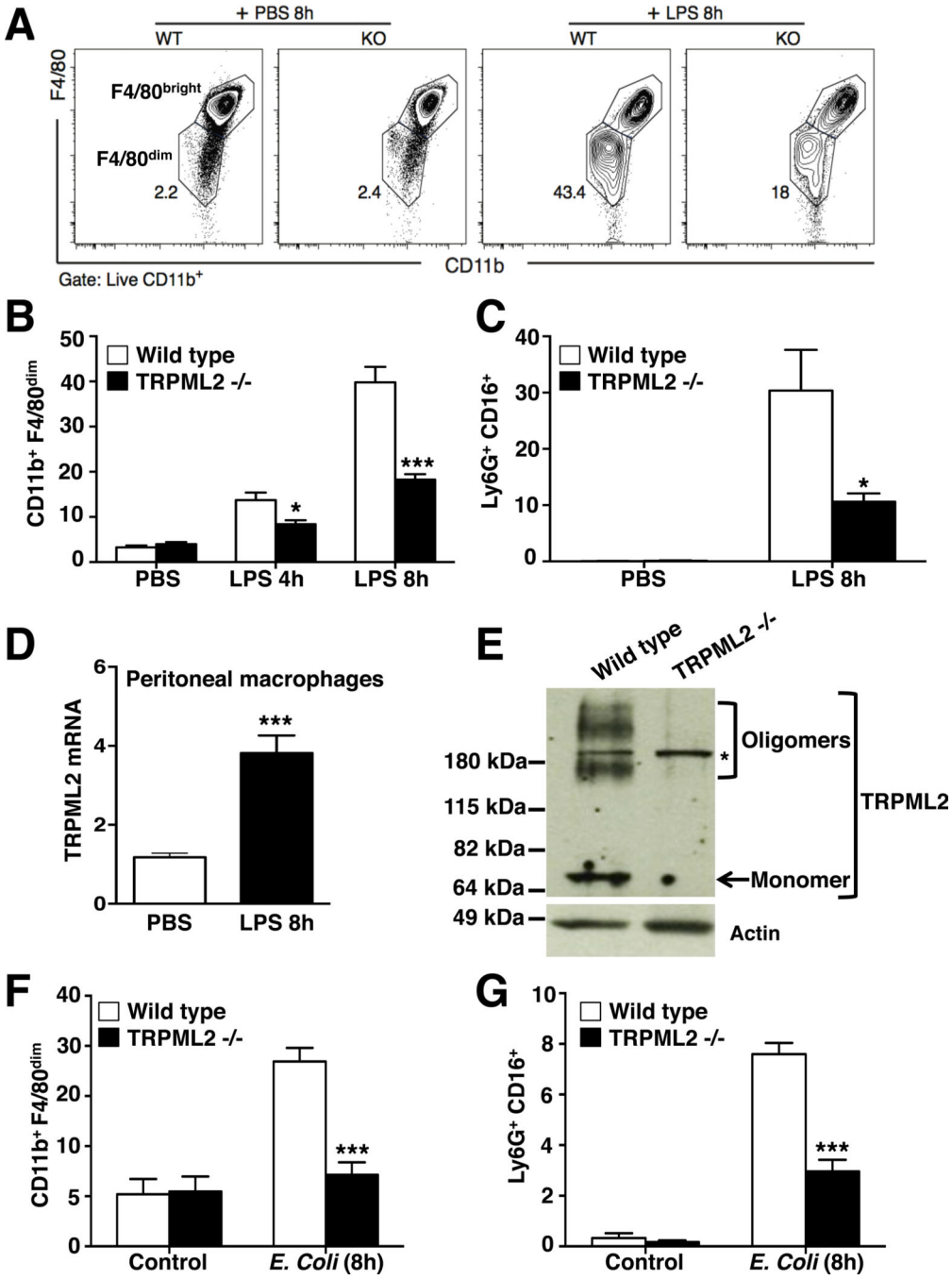

Figure 7. Macrophage migration is impaired in TRPML2 knockout mice

A. Flow cytometric analysis of $CD11b^{+}F4/80^{bright}$ (indicative of resident macrophages) and $CD11b^{+}F4/80^{dim}$ (indicative of recruited macrophages) peritoneal macrophages isolated from peritoneal fluid of WT and TRPML2 KO mice injected with saline or LPS for 8 hours. Numbers represent the $CD11b^{+}F4/80^{dim}$ percentage of CD11b positive cells. **B.** Graphical representation of percentage of $CD11b^{+}F4/80^{dim}$ cells from WT (white) and TRPML2 KO (black) mice injected with saline or LPS (0.5 μg/g) for 4 hours or 8 hours. Data are presented as means ± SD of at least three independent experiments (LPS 4h: n=4, LPS 8h: n=16,

saline: n=11). The data were analyzed using two-way ANOVA (**P* (LPS 4h)<0.05, ****P*(LPS 8h)<0.0005). **C.** Graphical representation of percentage of neutrophils ($Ly6G^+CD16^+$ cells) from WT (white) and TRPML2 KO (black) mice injected with saline or LPS (0.5 μg/g) for 8 hours. Data are presented as means ± SD of three independent experiments (LPS 8h: n=7, saline: n=5). The data were analyzed using two-way ANOVA (**P*<0.05). **D.** TRPML2 mRNA levels from peritoneal macrophages isolated from WT mice that were injected with saline or LPS. Statistical significance was determined by two-tailed unpaired Student's *t* test. Error bars represent SEM (n=13 for LPS group and n=7 for saline group, ****P*< 0.0001). **E.** TRPML2 protein levels in peritoneal macrophages extracted from WT and KO mouse were assessed by western blot. The predicted molecular weight for TRPML2 is approximately 65 kDa (arrow). TRPML2 oligomers run above the 180 kDA marker. The asterisk indicates an unspecific band recognized by our antibody. Actin (42 kDa) was used as a loading control. The shown image is a representative from three independent experiments. **F.** Graphical representation of percentage of $CD11b^+F4/80^{dim}$ cells from WT (white) and TRPML2 KO (black) mice injected with saline or live enterotoxigenic *Escherichia coli* (strain H10407) (5×10^7 CFUs) for 8 hours. Data are presented as means ± SD of two independent experiments (*E coli*: n=5, saline: n=3). The data were analyzed using two-way ANOVA (****P*<0.0005). **G.** Graphical representation of percentage of $Ly6G^+CD16^+$ cells from WT (white) and TRPML2 KO (black) mice injected with saline or live enterotoxigenic *Escherichia coli* (strain H10407) (5×10^7 CFUs) for 8 hours. Data are presented as means ± SD of two independent experiments (*E coli*: n=5, saline: n=3). The data were analyzed using two-way ANOVA (****P*<0.0005).

Table 1

Analysis of kidney function in TRPML2 knockout mice

	wild type n=11	**TRPML2−/− n=11**
BUN (mg/dL)	2802 ± 231	2705 ± 225.6
Ca2+ (mg/dL)	5.882 ± 0.7883	6.355 ± 0.3457
Creatinine (mg/dL)	57.2 ± 4.114	50.82 ± 4.091
Glucose (mg/dL)	49.36 ± 2.068	48.27 ± 2.446
Mg2+ (mg/dL)	59.78 ± 4.336	57.41 ± 4.825
phosphorous (mg/dL)	292.5 ± 26.21	238.6 ± 20.92
K+ (nmol/L)	184.8 ± 15.81	182.5 ± 16.71
Na+ (nmol/L)	110 ± 7.395	117 ± 7.469

Urine samples were collected from 3 months old female mice for urine panel analysis. WT (n=11) and KO (n=11) mouse were kept in metabolic cages for 24 h for urine collection. The data shown are means ± SEM.